

NASA/CR—1998-208869



Development of UV Optical Measurements of Nitric Oxide and Hydroxyl Radical at the Exit of High Pressure Gas Turbine Combustors

D.S. Liscinsky, B.A. Knight, and J.A. Shirley
United Technologies Research Center, East Hartford, Connecticut

Prepared under Contract NAS3-27593

National Aeronautics and
Space Administration

Lewis Research Center

December 1998

Acknowledgments

This contract was monitored by Dr. Chowen Chou Wey of the National Aeronautics and Space Administration's Lewis Research Center with funding provided by NASA's Atmospheric Effects of Aviation Project. The encouragement and active participation in technical discussions by Dr. Wey is greatly appreciated. The support and interest of Rich Neidzwiecki and the staff of the Combustion Branch at NASA Lewis Research Center is also gratefully acknowledged.

The assistance of Mr. C. Evans, Mr. A. Jennings, Mr. D. Kocum, Mr. R. Muth, and Mr. B. True of UTRC for the experimental section of this study is gratefully acknowledged. Helpful discussions with B.A. Woody of UTRC are also gratefully acknowledged.

Available from

NASA Center for Aerospace Information
7121 Standard Drive
Hanover, MD 21076
Price Code: A03

National Technical Information Service
5285 Port Royal Road
Springfield, VA 22100
Price Code: A03

Development of UV Optical Measurements of Nitric Oxide and Hydroxyl Radical at the Exit of High Pressure Gas Turbine Combustors

Final Report

(March 1995 to March 1998)

**Prepared by :
D.S. Liscinsky
B.A. Knight
J.A. Shirley**

**Program Manager:
M.F. Zabielski**

**United Technologies Research Center
East Hartford, CT 06108**

**Prepared for :
Chowen Chou Wey
NASA Lewis Research Center**

NASA Contract NAS3-27593

Abstract

Measurements of nitric oxide (NO) and hydroxyl radical (OH) have been made in a laboratory flat flame at pressures up to 30 atm using line-of-sight resonant absorption. Data are reported at equivalence ratios of 0.98 and 1.3 and pressures of 1, 5, 10, 20 and 30 atm. The performance of the *in-situ* UV absorption technique was assessed at these elevated pressures by comparing the measured absorption with those predicted by detailed theoretical spectroscopic models for NO and OH. Previous to this experiment the resonant models had not been verified at pressures greater than two atmospheres. Agreement within 25% was found between the measurements and predictions with only slight modification of the existing models for both NO and OH to account for line center shifting and pressure broadening. Continuum interference of hot oxygen (O₂) on the NO absorption spectra was not significant in the interpretation of the data.

The optical methods used in this study are distinct from laser-based diagnostics such as laser induced fluorescence and, hence, have the potential to provide independent verification of the laser-based measurements. The methodology is also of sufficient simplicity to be hardened into a portable optical measurement system that can be deployed in gas turbine engine test cells. A miniature fiber optic couple portable instrument is described.

Acknowledgements

This contract was monitored by Dr. Chowen Chou Wey of the National Aeronautic and Space Administration's Lewis Research Center with funding provided by NASA's Atmospheric Effects of Aviation Project. The encouragement and active participation in technical discussions by Dr. Wey is greatly appreciated. The support and interest of Rich Neidzwiecki and the staff of the Combustion Branch at NASA Lewis Research Center is also gratefully acknowledged.

The assistance of Mr. C. Evans, Mr. A. Jennings, Mr. D. Kocum, Mr. R. Muth, and Mr. B. True of UTRC for the experimental section of this study is gratefully acknowledged. Helpful discussions with B.A. Woody of UTRC are also gratefully acknowledged.

Table of Contents

<i>Development of UV Optical Measurements of Nitric Oxide and Hydroxyl Radical at the Exit of High Pressure Gas Turbine Combustors</i>	1
Abstract	2
Acknowledgements	3
List of Figures	5
List of Tables	5
Introduction	6
Background	6
Laboratory High Pressure Flame Facility	7
Burner Characterization	10
Nitric Oxide (NO) Optical Measurements	14
Basis for the Absorption Measurement	14
Instrumentation	15
Data Reduction	16
Comparison of Experimental and Predicted Concentrations (no flame condition)	17
Radial Temperature Profiles	18
Comparison of Experimental and Predicted NO Concentrations	19
Hydroxyl (OH) Optical Measurements	21
OH Model	22
Comparison of Experimental and Predicted OH Concentrations	23
Portable Instrument	27
Field Test of the Absorption Measurement Instrumentation	29
Conclusions	31
New Technology	31
Suggestions for Future Activities	32
References	33

List of Figures

Figure 1: High Pressure Chamber	7
Figure 2: Chimney/burner and Dome Assembly.....	7
Figure 3: Axial Cross Section of the High Pressure Combustion Chamber	8
Figure 4: Radial Cross Section of the High Pressure Combustion Chamber	8
Figure 5: Flat Flame Burner	9
Figure 6: Chimney and Burner Assembly.....	9
Figure 7: Laboratory Layout of the High Pressure Combustion Facility.....	10
Figure 8: Safety and Control System Schematic for the High Pressure Combustion Facility.....	10
Figure 9: Species Concentration Profiles at 5 Atmospheres.....	11
Figure 10: Species Concentration Profiles at 20 Atmospheres.....	12
Figure 11: Species Concentration Profiles at 10 Atmospheres with NO Seeding at 450 ppm.....	12
Figure 12: Species Concentration Profiles at 20 Atmospheres with NO Seeding at 300 ppm.....	12
Figure 13: Radial Temperature Profiles at $\Phi = 0.82$	13
Figure 14: Schematic of the in-situ line-of-sight measurement.....	14
Figure 15: UTRC water-cooled hollow cathode lamp (HCL).....	16
Figure 16: Nitric Oxide Emission spectra of the UTRC hollow cathode lamp	16
Figure 17: Measured NO Absorption Spectra at 15.6 atm.....	17
Figure 18: Model Predicted NO absorption spectra at 15.6 atm.....	18
Figure 19: Radial temperature profile at 5 atm and $\phi = 1.3$	19
Figure 20: NO absorption spectra at 30 atm and an equivalence ratio of 1.3.....	20
Figure 21: OH A-X(0,0) Transmission for an OH mole fraction of 0.003	22
Figure 22: OH A-X(0,0) Transmission for an OH mole fraction of 0.003	23
Figure 23: OH Emission spectra of the UTRC hollow cathode lamp	24
Figure 24: High Resolution OH Emission spectra of the UTRC hollow cathode lamp	24
Figure 25: OH Absorption Spectra at 30 atm and $\phi = 0.98$	25
Figure 26: Ocean Optics PC1000 installed in a Personal Computer	27
Figure 27: Absorption Spectra of NO obtained from a Static Cell with the PC1000	28
Figure 28: Model Prediction for 91.8ppm NO, $L = 18.6$ cm, FWHM = 1nm, 298 degK.....	28
Figure 29: OH Spectra obtained with the PC 1000 in a Laboratory Flame.....	29

List of Tables

Table 1: Comparison of Measured and Model Predictions vs. Pressure at Room Temperature..	18
Table 2: Comparison of Measured and Predicted Absorption.....	20
Table 3: Comparison of Measured and Predicted Absorption.....	21
Table 4: Comparison of Model Predictions with and without Line Center Shifting.....	21
Table 5: Comparison of Measured and Predicted Absorption.....	25
Table 6: Comparison of Measured and Predicted Absorption.....	26

Introduction

The purpose of this project was to develop *in-situ* optical methods for the measurement of nitric oxide (NO) and hydroxyl radical (OH) present at the exit of aircraft combustors. Future gas turbine combustor exit pressures may approach 60 atmospheres and 3000K making optical diagnostics attractive tools to assess emission performance and provide initial concentrations of these species for atmospheric models. However, before these methods can be used with confidence their accuracy must be verified. In order to achieve this goal, the performance of line-of-sight methods was assessed at pressures up to 30 atmospheres. This required obtaining spectroscopic information not readily found in the literature, namely, the effect of pressure on line center shifting and doppler broadening. With this information, spectroscopic models can be used to predict molecular absorption at elevated pressures. Furthermore, the absorption methods, which are line-of-sight, are distinct from laser-based diagnostics such as laser induced fluorescence and, hence, have the potential to provide independent verification of the laser-based measurements.

The project was divided into five (5) main tasks which are given below:

Task 1 - Facilities Preparation

Task 2 - Laboratory High Pressure Optical NO and OH Measurements

Task 3 - Portable Optical Instrument Design and Assembly

Task 4 - Engine Measurements of NO and OH at Lewis Research Center

Task 5 - Reporting

The results of these activities are described in this report.

Background

In 1979, under contract to the FAA, UTRC performed a detailed study of nitric oxide measurement techniques (Zabielski et al, 1980). The Task I report from that study thoroughly covered optical techniques for measuring NO by calibrating UV spectroscopic methods and comparing those results to those obtained by conventional extractive chemiluminescent instrumentation. As part of that investigation, a detailed theoretical spectroscopic model was developed and verified; however, experimental data at pressures greater than 2 atm were not acquired.

In 1993, as part of NASA's High Speed Research Program (SRP), the Atmospheric Effects of Stratospheric Aircraft (AESA) project was initiated. Concurrently, NASA's Advanced Subsonic Technology Program (ASTP) initiated a Subsonic Assessment (SASS). Both of these projects (collectively referred to as NASA's Atmospheric Effects of Aviation Project, AEAP) were aimed at establishing the effect of aircraft emissions on the atmosphere. Laboratory, modeling and atmospheric observations established NO and OH as important species emitted by aircraft. It was recognized that an improved knowledge of these species concentrations was required for input to atmospheric models in order to predict their effect on ozone trends and high altitude cloud formation.

In 1995 UTRC was awarded contract NAS3-2754 to develop optical methods to measure NO and OH. The results of that contract are summarized in this report.

Laboratory High Pressure Flame Facility

The laboratory high pressure flame facility consists of a UTRC designed high pressure chamber, control systems for gas flow and monitoring, a custom burner, and provisions for vertical translation of the burner. The assembled apparatus and associated components are shown in Figure 1 and Figure 2. Figure 3 and Figure 4 provide details of the interior structure. The chamber, built by Parr Instrument Company, is 61 cm long, 15.24 cm in diameter, and is certified for operation up to 68 atmospheres pressure while maintaining an outer shell temperature of 573K, according to the ASME Boiler Code. There are six optical ports that provide line-of-sight access located at three axial locations along the chamber axis. At the position where the burner is located, the ports provide 3.8 cm diameter clear optical viewing area. The dome of the chamber contains a bellows connected to a drive motor that allows the burner to be traversed 4 cm in the vertical direction inside a quartz chimney while the chamber is pressurized. The chimney is constructed of planar quartz windows supported by Pyroceram® machinable ceramic and are 41.28 cm in length and 0.318 cm thick. Combustion products from the up-fired burner exit the chamber through a heat exchanger that is maintained at 250F and 150 psi to avoid water condensation.

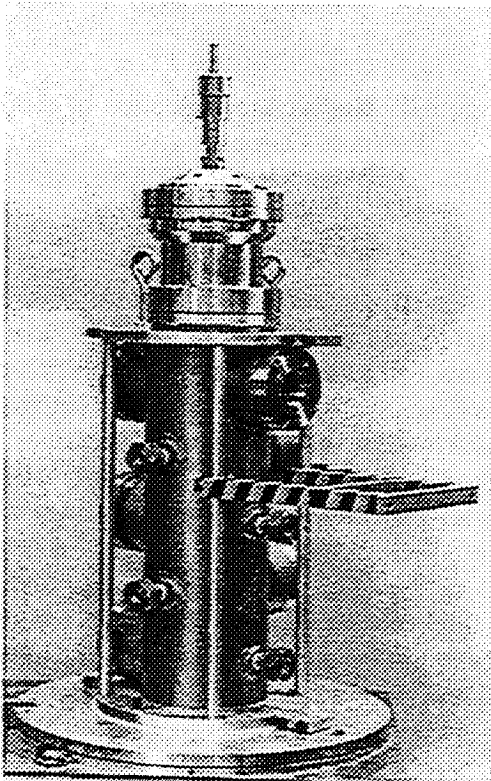


Figure 1: High Pressure Chamber

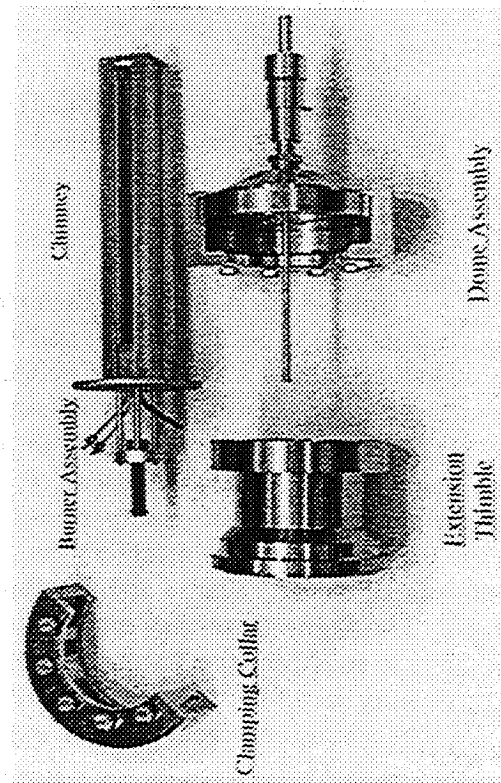


Figure 2: Chimney/burner and Dome Assembly

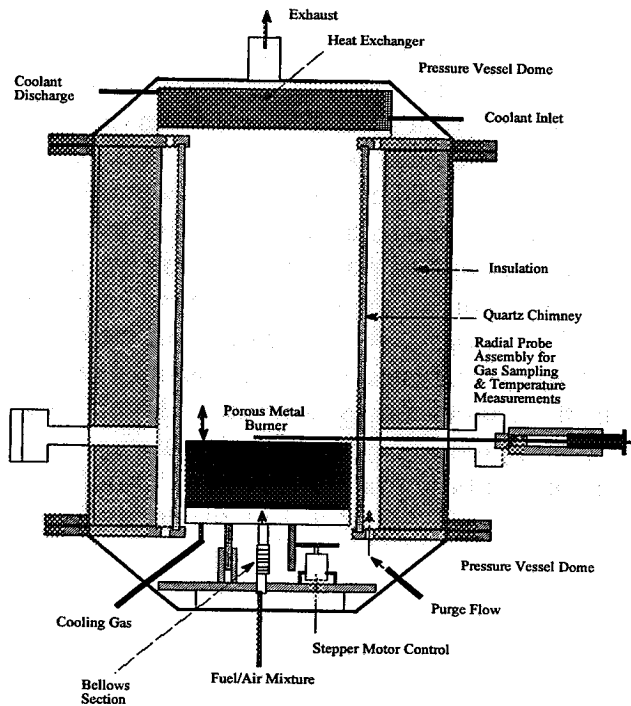


Figure 3: Axial Cross Section of the High Pressure Combustion Chamber

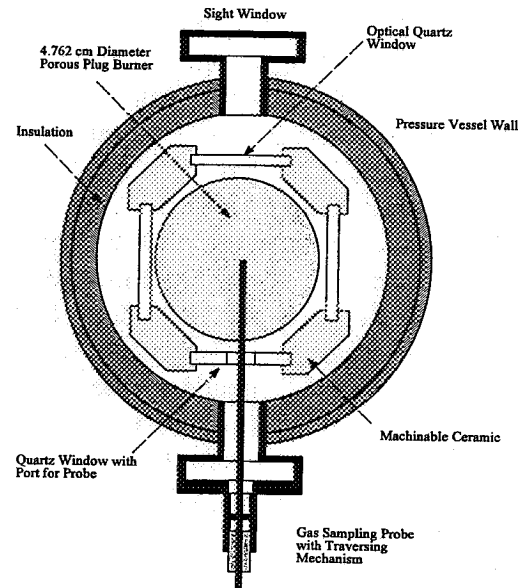


Figure 4: Radial Cross Section of the High Pressure Combustion Chamber

A water-cooled, 4.76 cm diameter, sintered porous copper surface, flat flame burner was used, as indicated in Figures 3 and 4. Figures 5 and 6 are photographs of the burner and associated chimney assembly, respectively. Previous experience had demonstrated the importance of maintaining a sufficiently high pressure drop across the flameholder (in this case the surface of the burner) in order to prevent resonance within the combustion chamber. This was accomplished with a series of screens and a packed bed of ceramic beads upstream of the porous surface. The uniformity of radial temperature and species profiles provided by the flat flame burner simplifies interpretation of the optical data and allows for modeling of a nearly 1-dimensional flame. Flame stabilization was achieved by matching the flow velocity and flame speed. The flame front was on the order of 1mm in thickness at 30 atm. Delicate control was required to maintain the flame as chamber pressure was increased since flame speed decreases significantly as pressure increases. Maintaining the flame over a range of pressures and fuel/air ratios was a complex process. The overall laboratory layout is shown in Figure 7.

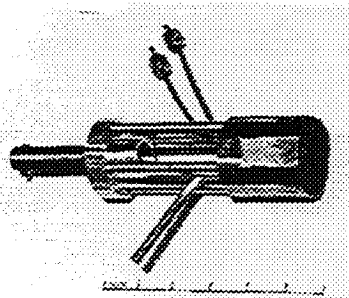


Figure 5: Flat Flame Burner

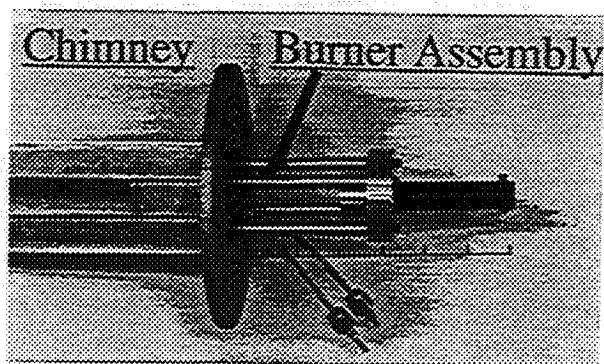


Figure 6: Chimney and Burner Assembly

Gas flows were metered from manifolded compressed gas cylinders using digital electronic mass flow controllers (Datametrics). The controllers were calibrated at pressure to 60 atm and provide maximum fuel and air flow rates of 150 and 1800 slpm, respectively, accurate to within $\pm 1/4\%$ of full scale (typically 100 slpm). Fuel (methane for all of the testing) and air to the burner are metered separately and mixed 100 diameters upstream of the burner. Air was metered separately for a purge flow outside the quartz chimney containing the flame. The purge flow was used to prevent exhaust gas recirculation in the region between the chimney and the chamber wall and, to some extent, for chamber cooling. In addition, provisions were made to meter seed gases through critical flow orifices into the fuel line. The chamber pressure was controlled with a pneumatically operated back-pressure regulator and all pressures were read to ± 0.1 psig using 12 diameter Heise gauges. Figure 8 is a schematic representation of the gas management system, controls and safety system discussed below.

For safety, a number of monitoring systems were in place that ensure: (1) sufficient water flow to the exhaust heat exchanger, (2) a preset temperature of the exhaust gas was not exceeded, (3) the chamber dome temperature did not exceed a preset value, and (4) gas leaks of either CO or fuel were detected (Sierra Monitor Corporation: CO detector with an alarm setting of 100 ppm, H_2/CH_4 detector with alarm settings of 1000 ppm for H_2 and 5000 ppm for CH_4 (the respective lower explosive limits are 40,000 ppm and 53,000 ppm for H_2 and CH_4)). In the event of loss of water or electrical power all systems shut down automatically. A back pressure regulator will open automatically if there is any loss of control pressure and vent the chamber pressure after shutting down all gas flows. In addition, an emergency shutdown switch was located on the control panel which shuts off fuel and air, reduces rig to atmospheric pressure and purges the rig with N_2 . Also, a 1" thick Plexiglas shield is located between the operators and the chamber and viewing of the flame is done via a video camera.

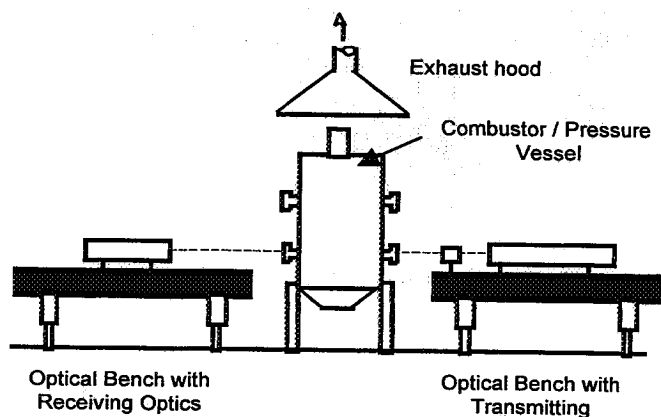


Figure 7: Laboratory Layout of the High Pressure Combustion Facility

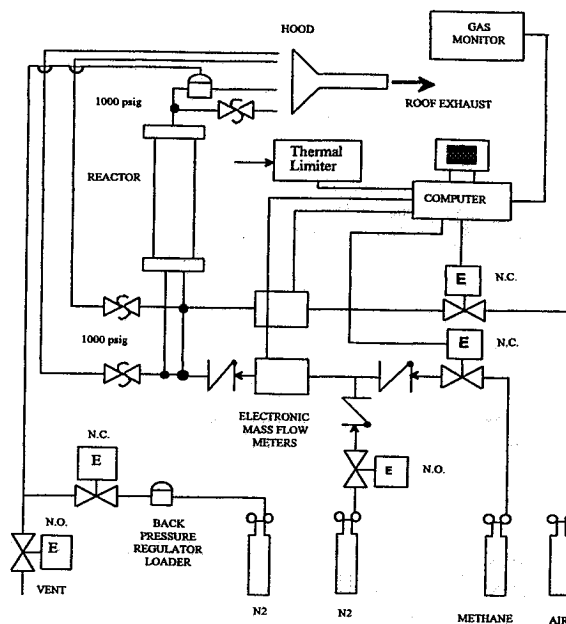


Figure 8: Safety and Control System Schematic for the High Pressure Combustion Facility

Burner Characterization

A conventional extractive gas analysis system was used to initially characterize the burner. The gas sampling system consisted of a 0.6 cm diameter, water-cooled, aerodynamic probe with a 0.025 cm diameter sampling orifice connected by a heated line to an emissions analysis rack that included a Beckman non-dispersive infrared (NDIR) analyzer for carbon monoxide (CO) (0-1000 ppmv range, 800 ppmv span gas), a Beckman NDIR carbon dioxide (CO₂) analyzer (0-5% range, 4% span gas), a Beckman paramagnetic oxygen (O₂) analyzer (0-25% range, 20.8% span gas), and a Thermo-Electron chemiluminescent analyzer for nitric oxide (NO) and oxides of nitrogen (NO_x) (0-1000 ppmv range, 80 ppm span). The pressurized cooling water for the probe was maintained at 125°C to prevent internal water condensation and the sample was dried using an ice bath prior to distribution to the suite of analyzers. Vertical profiles were obtained by moving the burner using a precision reversible motor drive indexed by a position transducer with the probe in a fixed position. Radial profiles were obtained by sliding the probe through a threaded collar which retained the probe in a fixed mount which was threaded and indexed into the pressure chamber wall. To accommodate the probe, one of the lower sight windows was replaced with a flange containing the probe assembly. Access to the combustion products was achieved through a 0.6 cm diameter hole in the quartz chimney (shown schematically in Figure 3 and Figure 4).

Data were acquired from the gas sampling probe at 1, 5, 10, 20, 25, and 30 atmospheres at various burner equivalence ratios as a function of radial position at a downstream location 2.5 cm

from the burner surface. This position was found to provide reasonable CO burnout without excessive thermal loss to the chimney; consequently, that location was chosen for all measurements acquired in this program. A comparison of the data obtained at 5, 10, and 20 atm and an equivalence ratio of 0.82 is shown in Figure 9, Figure 10 and Figure 11.

The gas sampling data obtained at all pressures indicated a very low level of NO (and NO_x), typically on the order of 25 ppm. In anticipation of the optical measurements, where it was hoped to achieve significant absorption with a single pass through the flame zone (4.8 cm pathlength), provision was made to increase NO levels with the addition of a metered flow of 1% NO in argon. Species profiles with NO seeding into the fuel flow at 10 and 20 atm are shown in Figure 9 and Figure 10. The NO seed level was 450 ppm and 300 ppm with levels slightly less measured in the flame. The species and temperature profiles were not affected by the addition of the seed because of the low mass addition necessary to augment the NO level.

The profiles shown in Figures 9-13 indicate that the species profiles over 75% of the burner diameter are very uniform. Near the chimney wall the values are affected by heat loss and some purge air flow leaking around the burner. These gradients are unavoidable in the present design but can be accounted for in the modeling of the optical results. In addition, the seed flow had no observable effect on these gradients.

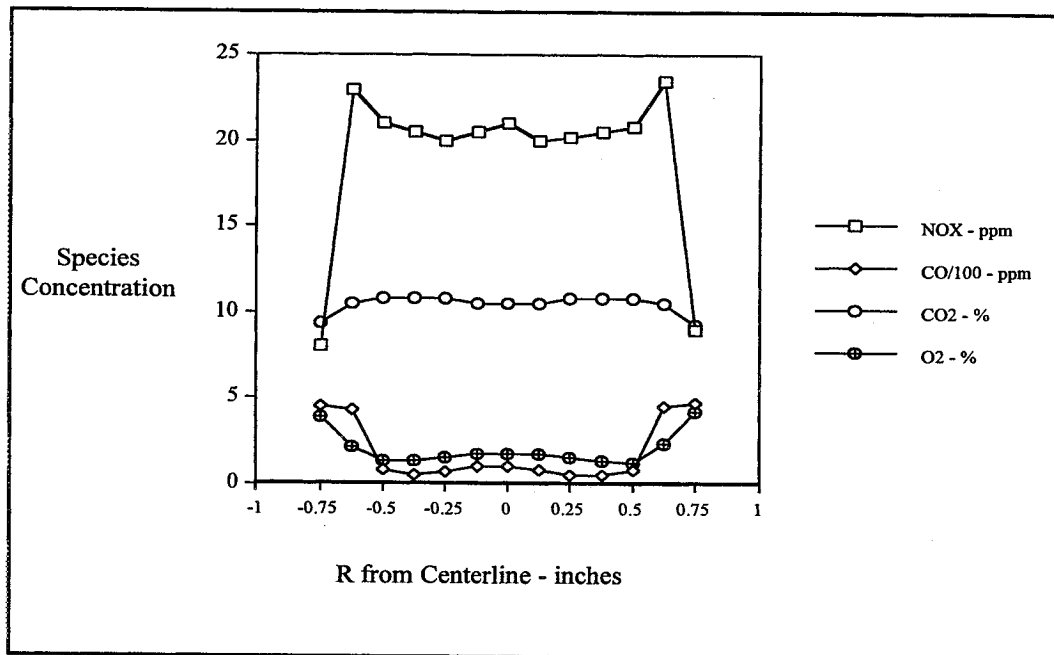


Figure 9: Species Concentration Profiles at 5 Atmospheres

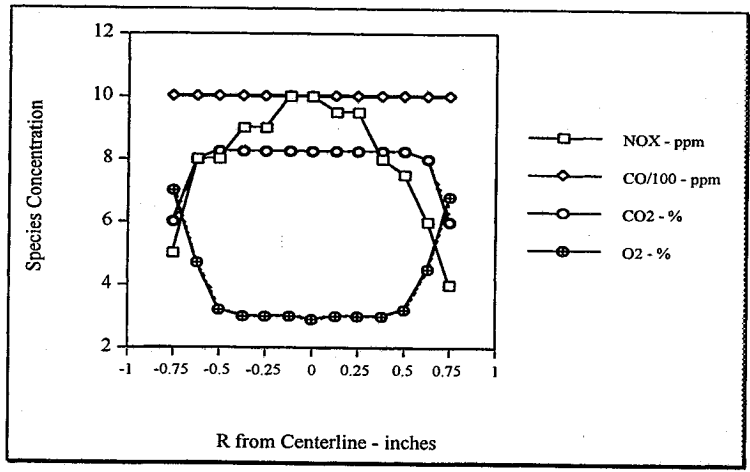


Figure 10: Species Concentration Profiles at 20 Atmospheres

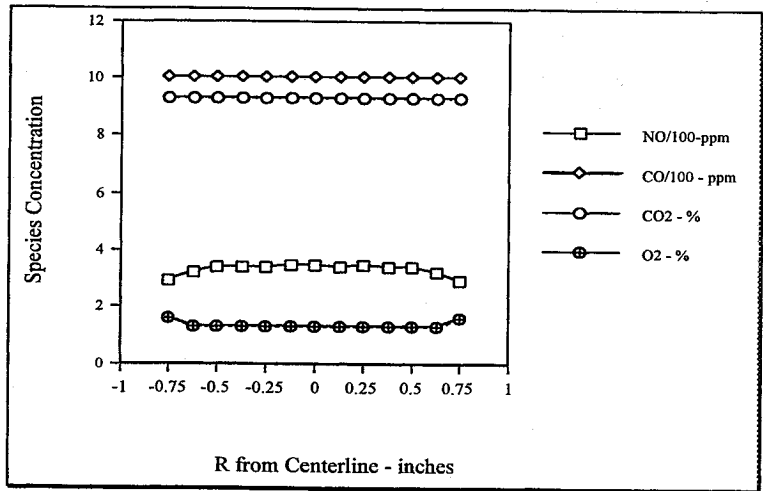


Figure 11: Species Concentration Profiles at 10 Atmospheres with NO Seeding at 450 ppm

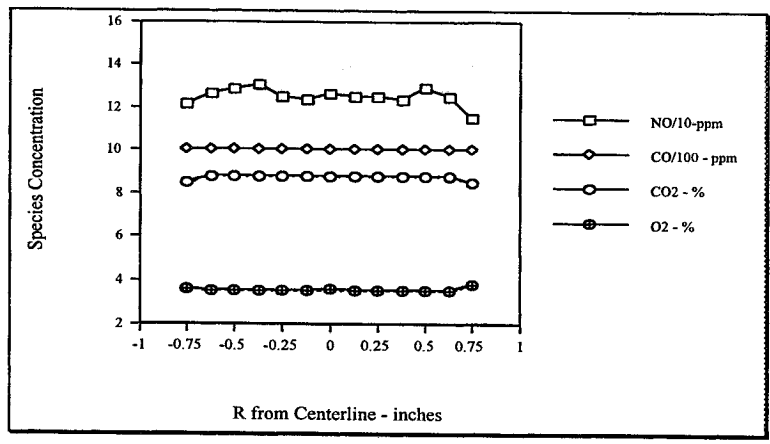


Figure 12: Species Concentration Profiles at 20 Atmospheres with NO Seeding at 300 ppm

To obtain temperature profiles in the flame zone, an ultra-fine wire platinum-platinum/13% rhodium thermocouple was used. The measuring bead of this thermocouple was formed by butt-welding 0.05 mm diameter wires, and locating the measuring junction 90 diameters from the 0.25 mm diameter lead wires. The measuring junction is coated with a mixture of 10% beryllium oxide – 90% yttrium oxide to minimize catalytic effects. The radiative loss of the measuring junction was estimated using the method described by Bradley et al (1961). The emissivity was 0.62 as previously reported (Zabielski et al, 1980). A fine wire thermocouple of this size was needed not only to minimize conductivity losses to the thermocouple support, but because the actual flame zone is very thin at high pressure (30 atm). This thermocouple probe has been manufactured by modifying a commercially available platinum-sheathed thermocouple probe assembly from Omega Engineering®. The sheath was removed from the probe assembly and the 0.25 mm diameter thermocouple wires exposed. These wires were inserted in a 25 mm long alumina sheath which was cemented to the end of the platinum sheath. The measuring junction consists of butt-welded 0.05 mm wires which are welded onto the support wires. This gave a measuring junction, which has a low thermal conductivity loss and a small time constant on the order of 15 milliseconds to respond to fluctuations in the flame. Although the thermocouple was used for steady-state temperature measurements, low thermal mass and low conductivity losses were important for accurate measurements in a high pressure flame where the reaction zone is physically compressed.

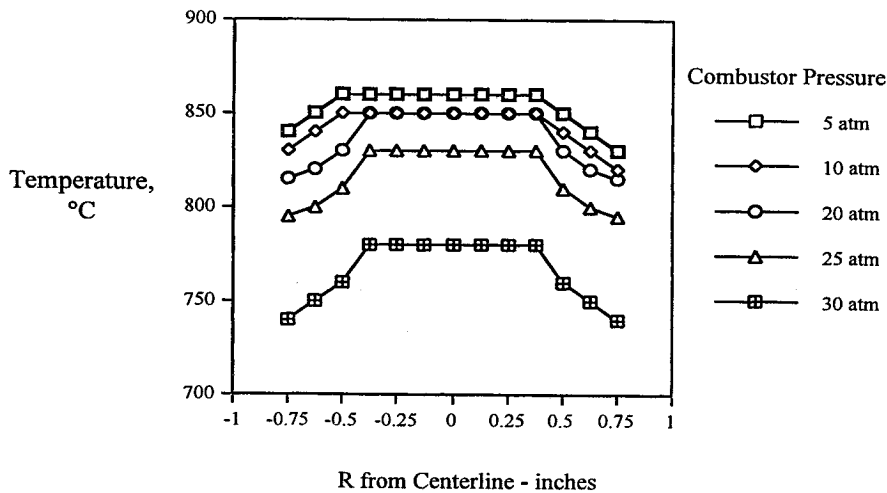


Figure 13: Radial Temperature Profiles at $\Phi = 0.82$

(NO seeding at 450 ppm and w/o radiation correction)

Nitric Oxide (NO) Optical Measurements

The method used for the in-situ optical measurement of NO concentration was line-of-sight UV resonant absorption, shown schematically in Figure 14. This is a classic molecular absorption technique which has been used by a variety of researchers (Davis, 1976; Few, 1977; Howard, 1990; Meinel, 1977; Zabielski, 1980), although always near atmospheric pressure. In this program, measurements were made at pressures up to 30 atm and the results were compared to model calculations based on the theoretical line-by-line absorption in the NO $\gamma(0,0)$ band. The primary advantage of this absorption technique is its inherent simplicity; however, in order to be quantitative, the temperature (and pressure) along the line-of-sight must also be known. In addition, the effects of pressure on the spectroscopy, namely line center shifting and doppler line broadening, must be correctly taken into account.

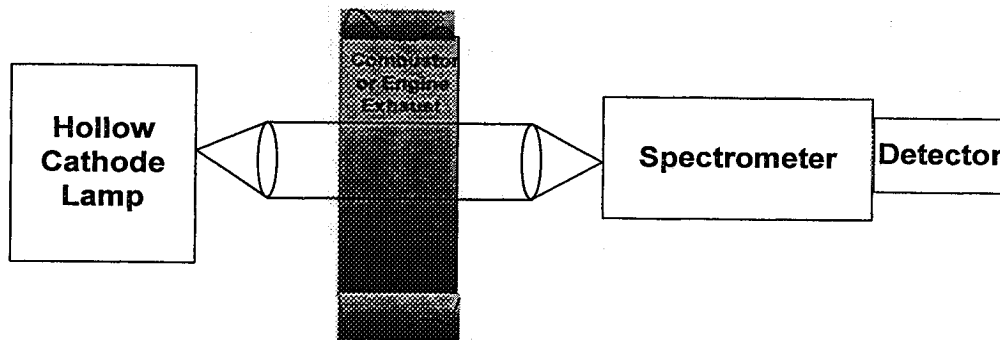


Figure 14: Schematic of the in-situ line-of-sight measurement

Basis for the Absorption Measurement

In its simplest form, the measured amount of absorption by an arrangement such as shown in Figure 14 follows a Beer-Lambert relationship:

$$\frac{I}{I_0} = e^{-\alpha c L} \quad (1)$$

where,

- I = final intensity
- I_0 = initial intensity
- α = absorption coefficient
- c = concentration
- L = pathlength

The intensity, or transmission, decays exponentially as pathlength increases or concentration increases and if α is significant, then absorption can be a very sensitive measurement of concentration. However α , although independent of I , c , and L , is dependent on wavenumber (ν)

and is a function of the absorption spectrum of the molecules in the optical path. The amount of absorption is inversely proportional to temperature, directly proportional to pressure and related to a line shape function which is affected by both temperature and pressure. For nitric oxide the absorption spectrum in the $\gamma(0,0)$ band has been studied extensively and can be theoretically calculated using a detailed model such as that discussed and developed by Zabielski et al (1980). The model produces computer-generated spectra that are convolved with an instrument slit function of arbitrary width. A Voigt line profile is used so that any pressure or temperature can be simulated. Initially, the model was developed and tested over a pressure range of 1 to 2.0 atm and a temperature range of 300 to 1900°K. The model was modified in this program to remove the high pressure limitation.

The use of a model, once validated, removes the need to experimentally generate calibration curves for the conditions of interest in order to interpret the measurements. Since generation of the empirical curves would be a very tedious task which would be instrument dependent, considerable effort has been expended to develop a suitable model (Davis et al, 1976; Few et al, 1977; Zabielski et al, 1980). The theoretical development will not be repeated here other than to show the transmission equation that is solved:

$$T(\nu) = I(\nu) \exp \left[-\frac{L}{\pi} \sum k_{\nu i}^0 \int_{-\infty}^{\infty} \frac{a' e^{-y^2} dy}{a'^2 + (\omega_i - \nu)^2} \right] \quad (2)$$

The essence of (2) is that the measured transmission $[T(\nu)]$ at some wavelength is a function of the source intensity $[I(\nu)]$, the pathlength (L), the line center Doppler absorption coefficient ($k_{\nu i}^0$), broadening parameter (a'), and wavenumber (ν). In other words the transmission is a function of the properties of the gas in the optical path, i.e. number density of absorbers, temperature and pressure, assuming a homogeneous path. (For further details and definitions of the theoretical model, see Zabielski et al, 1980). The model is used by providing the known optical path conditions and then calculating the transmissions for an estimated NO number density. The estimate is varied until the predicted and measured transmissions match. Only the $\gamma(0,0)$ band is described in the model.

In addition, the model was modified to include line center shifting. The shifting parameters determined by DiRosa and Hanson (1994) were used.

Instrumentation

The source of resonant NO radiation was a water-cooled hollow cathode lamp custom built at UTRC, shown in Figure 15. In the lamp, a glow discharge is created in air flowing through the lamp housing at a pressure of 5 to 10 torr. This pressure is maintained by a mechanical vacuum pump. A current of about 25 ma at 600 VDC is required to strike the lamp. A hollow cathode design is used to create a "spot" which is held in a fixed position and therefore

easily focused through a test section, in this case, the high pressure chamber. Discrete emission lines in the γ bands of NO are produced from the recombination of O and N atoms with N_2 and O_2 as shown in Figure 16 at low spectral resolution. Although a continuum source could also be used, by using a resonant source the signal-to-noise ratio is increased because the emitter radiation is matched, or resonant, with the absorber energy level.

The detection system used in this study consisted of a crossed Czerny-Turner design 0.275m focal length spectrometer (Jarrell-Ash Monospec 27) with a variable width entrance slit set at 25 μm , a 1200 groove/mm grating, a 1024 element array silicon diode detector (EG&G Princeton Applied Research model 1421), and a computer controlled interface (EG&G model 1461). This system is referred to as an optical multichannel analyzer (OMA®). The grating was used in first order and the detector was UV enhanced, intensified, and gateable. The spectral range used was 208 to 280 nm (0.07 nm/pixel spectral dispersion) and the measured spectral resolution was 0.3 nm (full-width-half-maximum (fwhm)). The output from the hollow cathode lamp was collimated into a 6 mm diameter beam and directed through the lower optical ports of the pressure chamber where it was focussed into a 10 m long 400 μm diameter fiber optic cable. Light exiting the opposite end of the cable was then focussed on the entrance slit of the spectrometer.

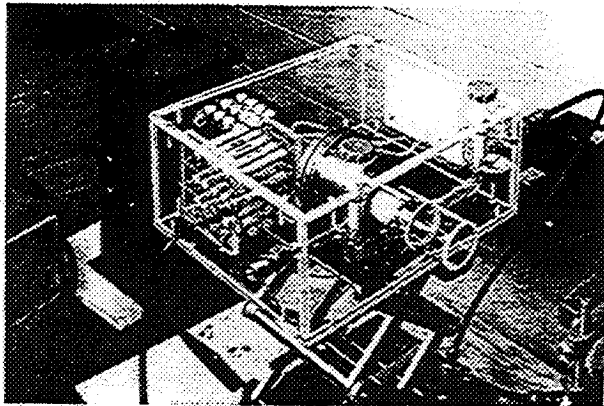


Figure 15: UTRC water-cooled hollow cathode lamp (HCL)

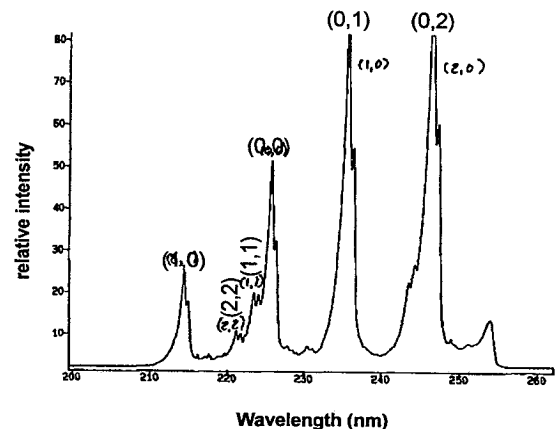


Figure 16: Nitric Oxide Emission spectra of the UTRC hollow cathode lamp (shown at spectral resolution typical of that used for the measurements in this program)

Data Reduction

Data reduction to yield the line-of-sight NO concentration for uniform temperature and pressure conditions was done as follows: A reference spectra (I_0) was obtained without NO present followed by acquisition of a test spectra with NO present. In low resolution, absorption at 226.2 nm corresponding to the 2nd rotational bandhead of the $\gamma(0,0)$ transition provides a convenient measurement of the number of absorbing molecules in the optical path. The

absorption of the intensity at the $\gamma(1,1)$ band (223.9 nm), or the $\gamma(2,2)$ band (221.6 nm), provide a means for treating spurious continuum attenuation due to window fogging, variation in source intensity, and other broadband absorption and is used to determine the reference (I_0) $\gamma(0,0)$ intensity. In the flame these higher electronic-vibrational energy states are not significantly populated and therefore the probability of a change in signal level due to absorption by NO molecules is very small relative to the ground state (0,0). This intrinsic monitor of experimental conditions, which the higher energy levels offer, is an advantage of this method, especially in harsh field environments.

The measured transmission at the $\gamma(0,0)$ band was computed by performing a baseline correction (subtraction) using a linear fit through the "flat" regions from around 220nm to 240 nm. The ratio of the intensity at the reference condition (R1) was computed as $I_{(0,0)} / I_{(1,1)}$ or $I_{(0,0)} / I_{(2,2)}$ and similarly the ratio at the test condition (R2). The measured transmittance (I/I_0) is then simply $R2/R1$.

Comparison of Experimental and Predicted Concentrations (no flame condition)

Experiments without a flame were performed to establish confidence in the measurement technique compared to model calculations. In Figure 17 and Figure 18, the experimentally measured and predicted spectra are respectively shown at equivalent conditions: pressure = 15.6 atm, temperature = 293°K, pathlength = 4.76 cm, fwhm = 0.3 nm and NO concentration of 91 ppmv. The chamber was thoroughly purged with the seed gas (91 ppmv NO in N_2) and then pressurized to 26 atm. Data were acquired at several pressures as the chamber was vented. As seen in Figure 17 the ground state absorption near 226 nm results in a decrease in transmission relative to the reference condition (zero ppm NO). The observed absorption is about 70%, similar to that shown by the model prediction for these conditions which is plotted in Figure 18. In Table 1, the results of a series of measurements made at pressures from 5 to 26 atm are compared to model predictions with good agreement, especially considering the relatively short pathlength.

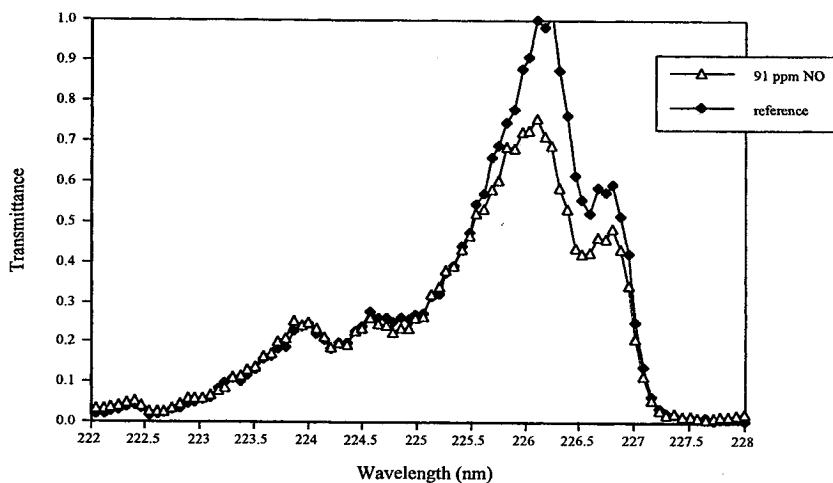


Figure 17: Measured NO Absorption Spectra at 15.6 atm (pathlength = 4.76 cm, fwhm of 0.3nm, 293K, 91 ppm NO)

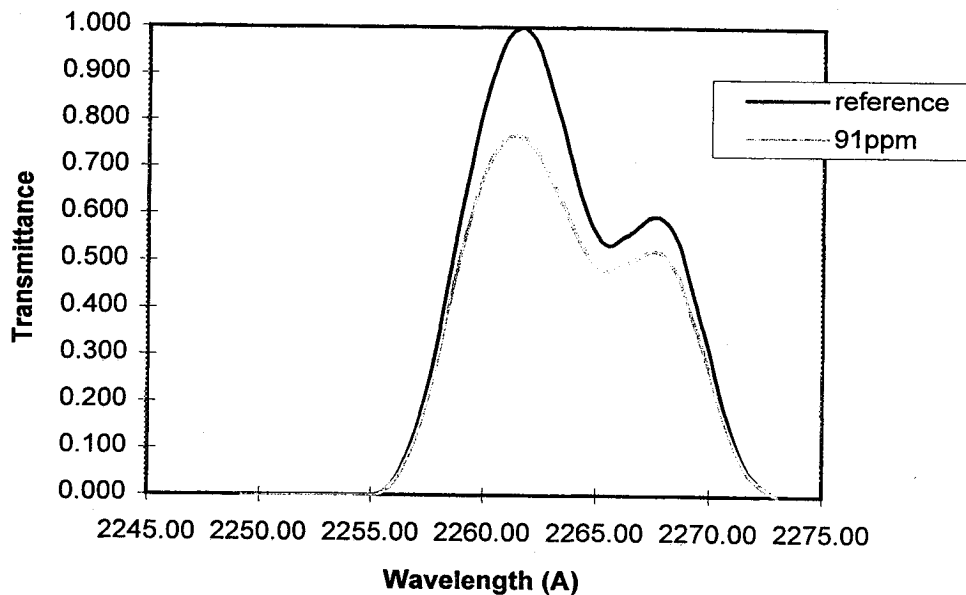


Figure 18: Model Predicted NO absorption spectra at 15.6 atm (pathlength = 4.76 cm, fwhm of 0.3nm, 293K, 91 ppm NO)

pressure (atm)	measured I/I ₀	predicted I/I ₀	% error *
26.0	.665	.679	5.1
21.6	.690	.711	8.1
15.6	.755	.765	4.7
10.0	.807	.828	12
5.0	.875	.897	18.6

Table 1: Comparison of Measured and Model Predictions vs. Pressure at Room Temperature (pathlength = 4.76 cm, fwhm of 0.3 nm, 293°K , 91 ppm NO)
 (* % error = 1 - [ln_{predicted}/ln_{measured}])

Radial Temperature Profiles

In order to interpret the line of sight absorption measurements in the flame, the temperature along the optical path must be known in order to compute the optical depth (number of molecules/cm² = 2.69E19*P*T*c*L) for input to the model. Since the model computes transmission for a homogeneous path, if the temperature is not uniform along the optical path, the pathlength must be modeled as zones. The output of each zone becomes the input for next zone so that the transmission is the multiplication of the transmissions computed for each zone. For the comparisons shown in this report, the radial temperature profiles were modeled typically with three (3) zones.

Additional temperature measurements beyond those shown previously in Figure 13 were acquired for application to the spectroscopic data. A beryllium/yttrium oxide coated fine wire Type R thermocouple (described previously in the Burner Characterization section) was used to measure the axial (downstream) profile on the burner centerline as a function of vessel pressure. Radial profiles were also acquired at 5 and 10 atm and 5.6 mm above the burner surface (the location chosen for the absorption measurement). Temperature measurements were also made at several equivalence ratios although spectroscopic data was only acquired at $\phi = 0.98$ and $\phi = 1.3$. A plot of the radiation corrected radial temperatures at 5 atm are shown in Figure 19 (zero being the midpoint of the burner). As mentioned above, details of the radiation correction can be found in Bradley (1961).

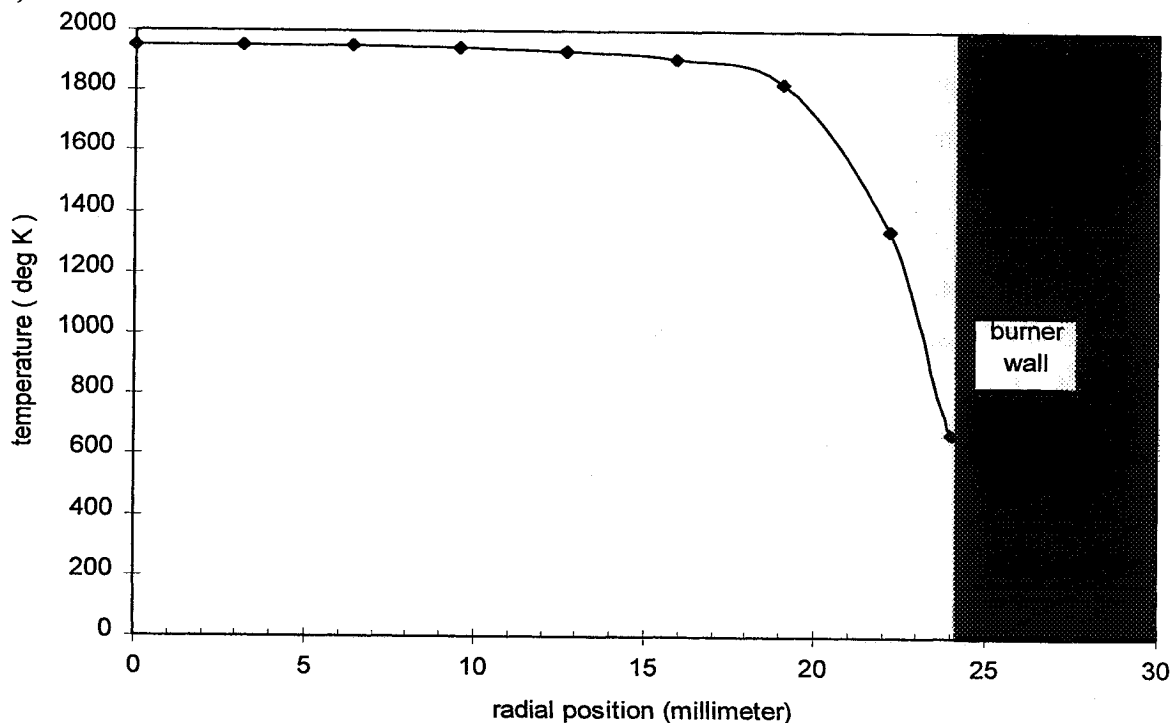


Figure 19: Radial temperature profile at 5 atm and $\phi = 1.3$

Comparison of Experimental and Predicted NO Concentrations

NO absorption spectra were acquired at pressures of 5, 10, 20 and 30 atm and an equivalence ratio of 1.3. It was found that burner operation was more robust with the fuel rich mixture, therefore this condition was used to provide the first data set for comparison with the computer model. For all cases exhaust emission data were also collected consisting of CO, CO₂, O₂, NO, NO_x for comparison purposes and to verify the actual flow conditions. NO seeding was performed at each test conditions to increase the NO signal level.

The absorption spectra at 30 atm is shown in Figure 20 between 220 and 240 nm. The $\gamma(2,2)$, $\gamma(1,1)$, $\gamma(0,0)$, and $\gamma(0,1)$ bands are indicated. Table 2 summarizes the results for this test

series. The absorptions predicted by the computer model calculations are also included. Agreement is seen to be within 32% for all cases but averages 20% overall (note that consistent with previously defined error equation (Zabielski, 1980) the % Error = $1 - (\ln [I/I_0] \text{ predicted}) / (\ln [I/I_0] \text{ measured})$). Although in this data set it appears that the measured absorption is generally greater than expected, it should be emphasized that this is reasonable agreement considering the short pathlength, the temperature measurement uncertainties, and the approximation of the temperature profile using only 3 zones. The goal for these measurement was an overall 25% agreement.

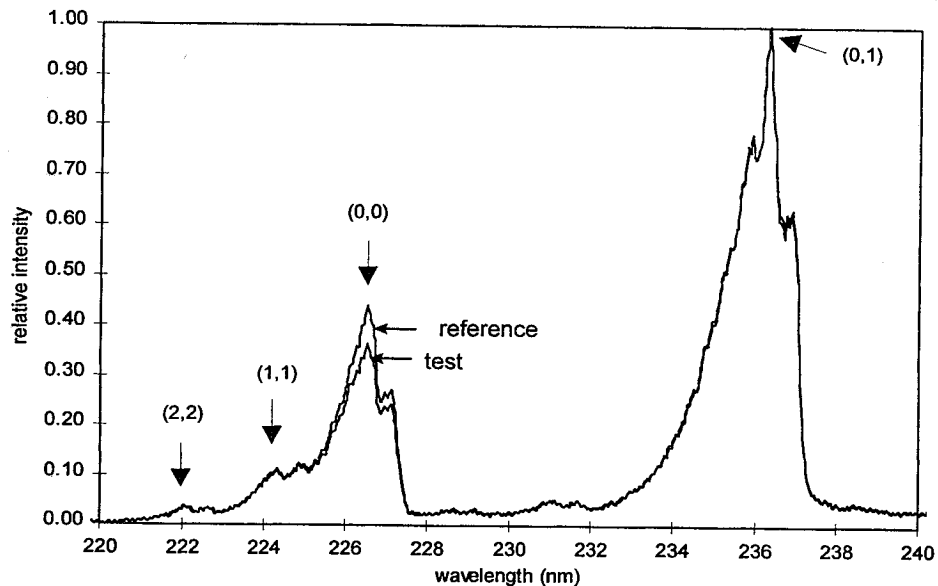


Figure 20: NO absorption spectra at 30 atm and an equivalence ratio of 1.3 (pathlength = 4.76 cm, fwhm of 0.3 nm, centerline temperature of 1612°K)

Pressure (atm)	Temperature (°K)	Measured NO _x (ppm)	Measured I / I ₀	Predicted I / I ₀	% Error
5	1930	140	.983	.987	22.5
10	1832	270	.952	.945	-13.5
20	1729	136	.901	.911	10.5
30	1612	114	.845	.892	31.8

Table 2: Comparison of Measured and Predicted Absorption (pathlength = 47.6 mm, FWHM = 0.3nm, $\phi = 1.3$)

A second set of data taken at an equivalence ratio of 0.98 and 5, 10, 20, and 30 atm is compared in Table 3. Although there has been concern regarding spectral interference from other species such as oxygen at pressures above 10 atm (Chang et al, 1992), the error in the

comparison of measured and predicted absorptions is seen to be on the order of 10% except for the 20 atm case. The error at this pressure was probably due to variations in the burner mass flows. Data were not collected at lower equivalence ratios to further explore oxygen interference at higher concentrations. It appears that at this spectral resolution (fwhm = 0.3 nm) and a pressure of 30 atm there is good agreement between measured and predicted results without accounting for interferences from other species.

Pressure (atm)	Temperature (°K)	Measured NO _x (ppm)	Measured I / I _o	Predicted I / I _o	% Error
5	1932	523	.959	.960	2.5
10	1832	640	.915	.920	6.1
20	1729	772	.888	.820	-67.1
30	1612	904	.669	.690	7.7

Table 3: Comparison of Measured and Predicted Absorption (pathlength = 47.6 mm, FWHM = 0.3nm, $\phi = 0.98$)

In order to determine the importance of line center shifting to this low resolution measurement method, calculations were performed with and without line center shifting. Table 4 gives this comparison, which shows that up to 30 atmospheres pressure, line center shifting is not a critical parameter.

Pressure (atm)	I / I _o with Line Center Shift	I / I _o without Line Center Shift
5	.9868	.9879
10	.9457	.9482
20	.9110	.9129
30	.8916	.8933

Table 4: Comparison of Model Predictions with and without Line Center Shifting (pathlength = 47.6 mm, FWHM = 0.3nm, $\phi = 1.3$)

Hydroxyl (OH) Optical Measurements

The absorption of radiation by the $A^2\Sigma-X^2\Pi(0,0)$ band of OH was measured using the same optical arrangement as shown previously for NO in Figure 14. The hollow cathode lamp was made to emit a resonant spectrum of OH by flowing water saturated argon through the discharge. The spectrometer was tuned to the 300 to 330 nm region. Data were collected at an equivalence ratios of 0.98 and 1.3 at pressures of 5, 10, 20, and 30 atm and compared to the predictions of a spectroscopic model for OH.

OH Model

The computer model incorporates the best available data for Einstein transition probabilities, energy levels and linewidths. The calculations of Goldman and Gillis (1981) have been used for the Einstein coefficients. These data were also used by Rea (1991). Rather than use Goldman and Gillis' data for the energy levels, the more accurate high resolution 1 m Fourier transform spectral measurements of Stark, Brault and Abrams (1994) are used. The measurements of Rea (1991, 1987) were used for the pressure broadening coefficients. Carter et al (1990) have tabulated Rea's data for the important collision partners in post flame combustion gases. These data are used with equilibrium calculations to determine the mole fraction of collision partners in the post flame combustion gases, to calculate a Voigt lineshape function, which is used with the linestrength to calculate the absorption (Goldman and Gillis, 1981; Rea, 1991).

A model calculation, assuming a flat continuum lamp spectral distribution, for an OH concentration of 300 ppmv (2000°K and 4.76 cm pathlength) at 1 atm is shown in Figure 21 and at 20 atm in Figure 22. A significant increase in absorption is predicted as pressure increases. The high degree of absorption is not a problem, however, since equilibrium concentrations of OH will be at least an order of magnitude less for the flame conditions that were studied.

The model is used in a similar fashion to the NO model. The known optical path conditions are provided and the OH concentration is "guessed" until the predicted and measured transmittances match. The measurements were made at much lower resolution than that plotted in Figure 21 and Figure 22. Therefore, as in the NO model, the computed single line intensities are convolved at the fwhm of the data in order to compare the measurements and predictions.

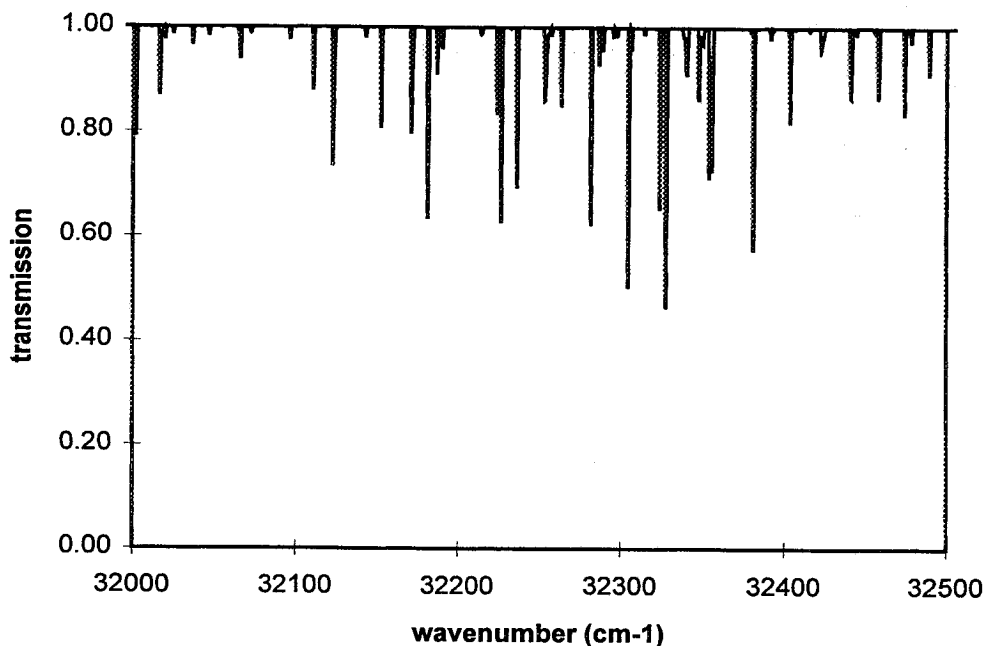


Figure 21: OH A-X(0,0) Transmission for an OH mole fraction of 0.003
(1 atm, 2000°K , L = 4.76 cm)

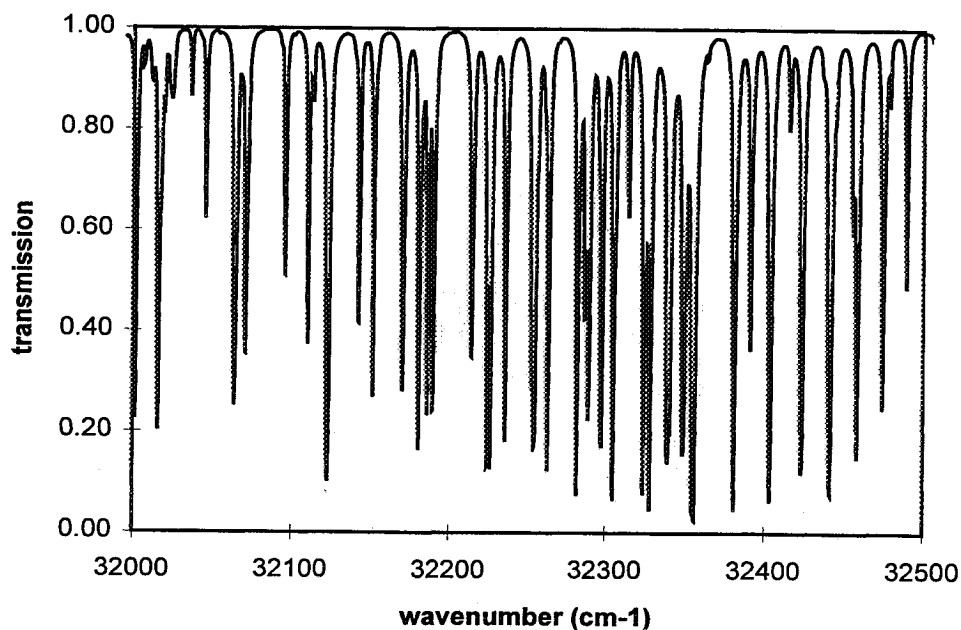


Figure 22: OH A-X(0,0) Transmission for an OH mole fraction of 0.003
(20 atm, 2000°K , L = 4.76 cm)

Comparison of Experimental and Predicted OH Concentrations

Measurements were made with the same instrument configuration in Figure 14. The emission spectra of the OH resonant source is shown in Figure 23 at the spectral resolution used for the data reported below. No individual lines are resolved. However, the source line intensity distribution of the hollow cathode lamp was measured in high resolution to resolve individual lines in order to calibrate the OH computer model. The OH emission was produced in the lamp shown in Figure 24. As previously stated, instead of flowing air into the lamp as was done for producing NO emission, argon (Ar) was bubbled through water and flowed into the lamp. The water in this saturated gas mixture dissociated into electronically excited OH and other species to produce the characteristic OH lines. A portion of the high resolution spectra is shown in Figure 25. These measurements were performed with a 1.5 meter spectrometer which was not portable and not available for the high pressure measurements.

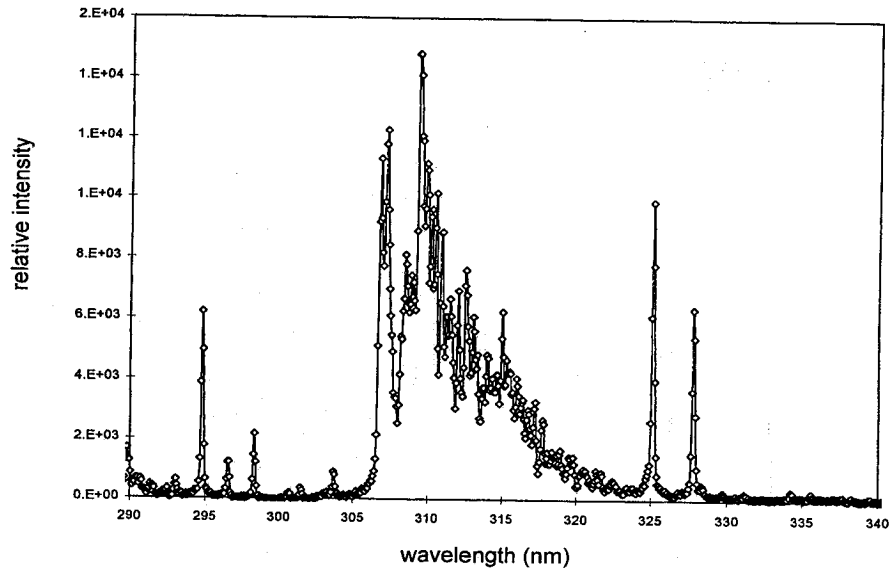


Figure 23: OH Emission spectra of the UTRC hollow cathode lamp (shown at spectral resolution used for the measurements in this program)

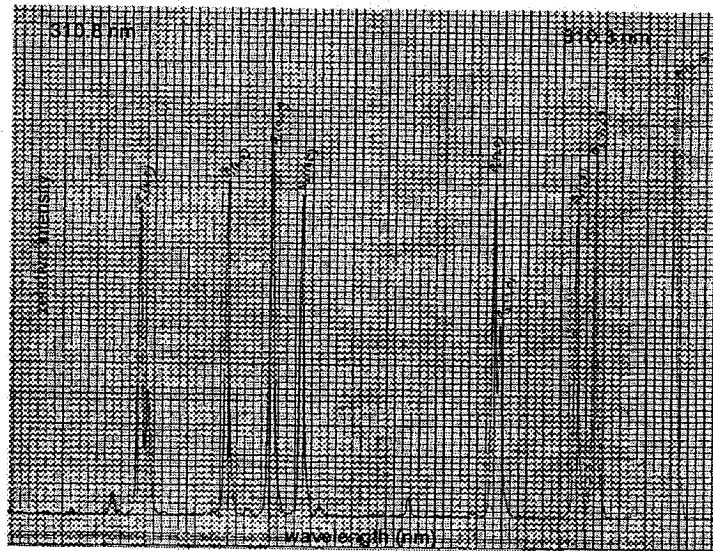


Figure 24: High Resolution OH Emission spectra of the UTRC hollow cathode lamp (fwhm = 0.0018nm)

In Figure 25 the absorption spectra is shown at 30 atm for a near stoichiometric flame. Significant absorption is observed for practically all lines, which was typical of all cases that were studied. Spectra like these were acquired at 5, 10, 20, and 30 atm for both $\phi=0.98$ and $\phi=1.3$ flames. The spectra were analyzed at several wavelengths for comparison to model calculations, but 310nm was used in all the results that will be presented. The equilibrium concentrations were calculated with the Sandia Chemkin code for constant temperature and pressure and used as input to the model to predict I/I_0 . The predictions are compared to the

measured absorptions in the following tables. The errors are also shown. (Note that the % error is calculated as shown on page 20).

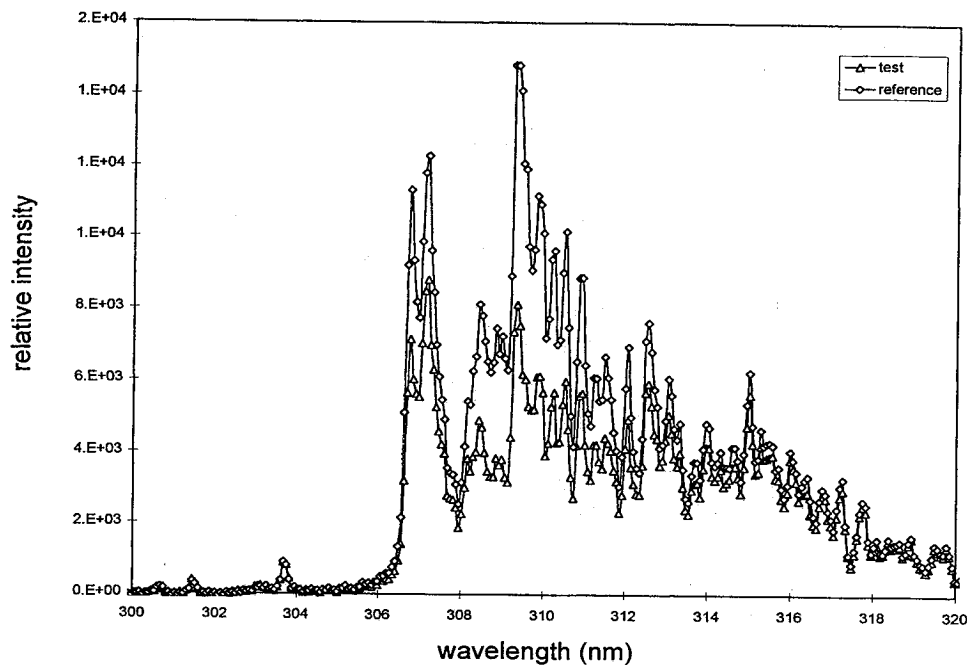


Figure 25: OH Absorption Spectra at 30 atm and $\phi = 0.98$
(fwhm = 0.3nm)

Results are compared for the $\phi = 1.3$ flame in Table 5. Like the NO comparison the predicted absorptions were calculated by dividing the temperature profile into 3 zones. Reasonable agreement was obtained.

Pressure (atm)	Temperature ($^{\circ}\text{K}$)	Equilibrium OH (ppm)	Measured I / I _o	Predicted I / I _o	% Error
5	1930	140	.983	.987	22.5
10	1832	270	.952	.945	-13.5
20	1729	136	.901	.911	10.5
30	1612	114	.845	.892	31.8

Table 5: Comparison of Measured and Predicted Absorption
(pathlength = 47.6 mm, FWHM = 0.3nm, $\phi = 1.3$)

Results are compared for the $\phi = 0.98$ flame in Table 6. It was found for these flames that use of the measured temperatures did not give good agreement. Therefore, what is shown in Table 6 are predictions near the maximum flame temperature that would be expected and how a 100°K variation in temperature affects the comparisons. Clearly a small change in assumed temperature can result in either good or poor agreement between the predicted and measured values. Therefore, although reasonable agreement is obtained, more accurate measurement of the temperature profile is needed to further to reduce the overall uncertainties.

pressure atm	temperature K	predicted I / I ₀	measured I / I ₀	% error
5	2002	0.770	0.874	-94.1
5	1919	0.865	0.874	-7.7
10	2000	0.798	0.793	2.7
10	1900	0.925	0.793	66.4
20	2189	0.686	0.689	-1.2
20	1989	0.924	0.689	78.8
30	2189	0.730	0.547	47.8
30	1989	0.936	0.547	89.0

Table 6: Comparison of Measured and Predicted Absorption
(pathlength = 47.6 mm, FWHM = 0.3nm, $\phi = 1.3$)

Portable Instrument

Although all of the optical measurements reported in the previous sections were obtained with a conventional laboratory spectrometer, effort to develop a portable instrument was expended in this program. Field measurements are of importance to obtain measurements under actual engine operating conditions and therefore a small easily deployed instrument was of interest. With this goal in mind, a small laboratory spectrometer used for this program was chosen to have spectral resolution comparable to what which might be expected to be deployable, i.e. a 1.5 meter spectrometer, although available, was not considered deployable.

A commercially available miniature fiber optic plug-in spectrometer (PC1000) from Ocean Optics was evaluated for use in this program. This low-cost spectrometer is based on a 1024-element linear CCD-array which is coupled via an SMA 905 connector to a fiber optic. The NEC 1024-element linear CCD-array silicon detector is responsive from 200-1000 nm with a signal-to-noise ratio of 1000:1. The optical design is based on a miniature crossed Czerny-Turner spectrometer. The grating in the unit used had 1800 lines/mm and 50 μ m slits which provided a fwhm resolution of 1.0nm (higher resolution options are now available). The detector signal can be integrated from 8 milliseconds to 4 seconds with the sampling rate and all other data acquisition variables programmable by software provided with the unit. The spectrometer is mounted on a half-length, 500 kHz ISA-bus A/D card and conveniently installs into an ISA-bus slot in a standard personal computer as shown in Figure 26.

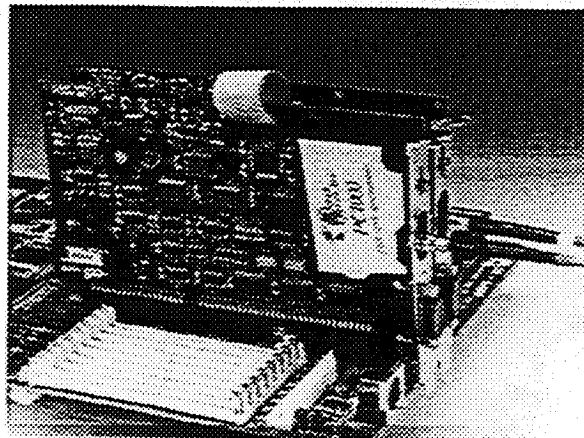


Figure 26: Ocean Optics PC1000 installed in a Personal Computer

The PC1000 was tested using an 18 cm long static cell to measure absorption for a calibrated mixture of NO in nitrogen. The spectra obtained for a 91.8 ppm concentration of NO is shown in Figure 27. Although the spectral resolution is at least 3 times less than the laboratory instrument, absorption is still indicated for the $\gamma(0,0)$ band near 226nm and the (0,1) band near 215nm. Even at this "low" resolution, reasonable agreement with the model predicted I/I₀ is obtained. The model predicted absorption is shown in Figure 28 . When baseline corrected the experimental and predicted I/I₀ values are within 5%.

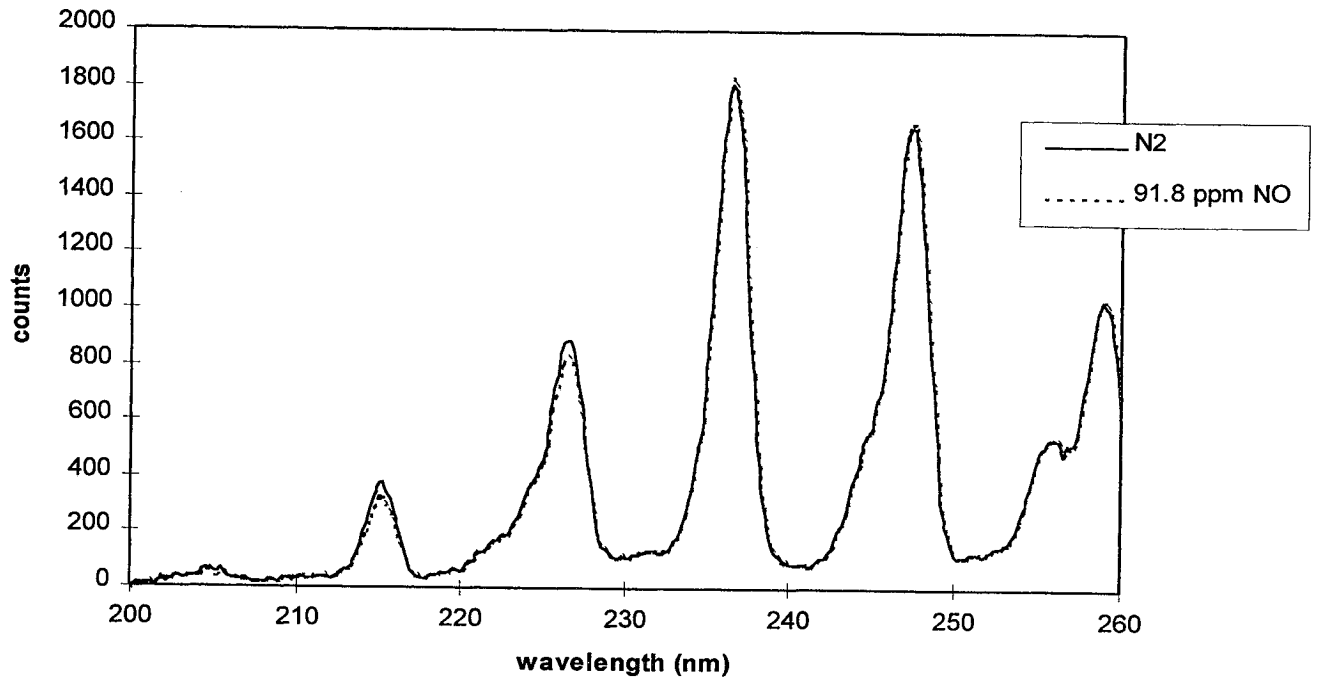


Figure 27: Absorption Spectra of NO obtained from a Static Cell with the PC1000 (L = 18.6cm, fwhm = 1nm, 91.8 ppm NO)

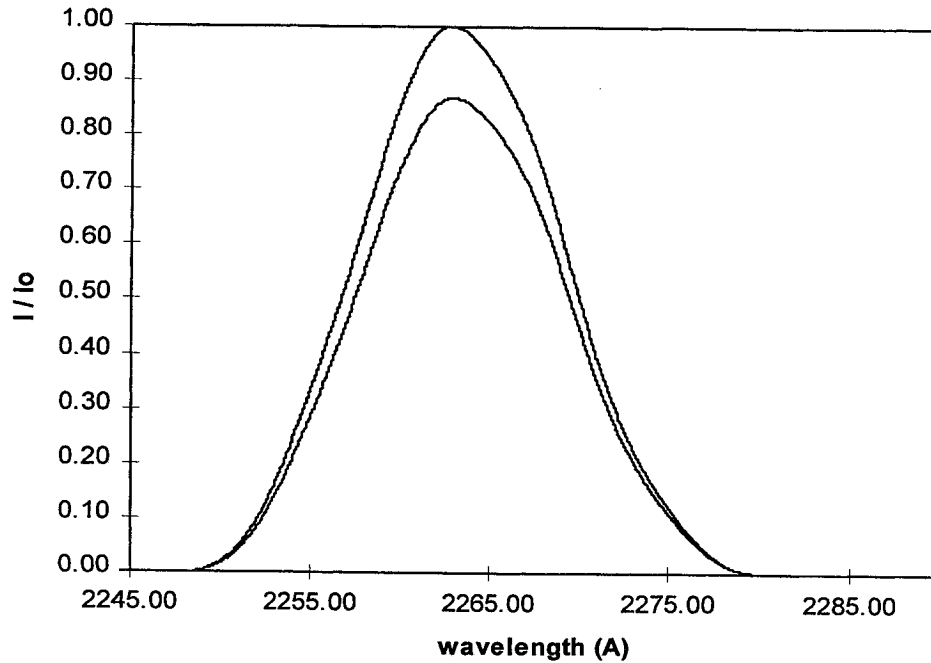


Figure 28: Model Prediction for 91.8 ppm NO, L = 18.6 cm, FWHM = 1nm, 298°K

An OH spectra obtained with the PC 1000 from a flat flame burner is shown in Figure 29. The modeling of this low resolution spectra requires a detailed accounting of the emission of the individual line of the lamp, the effect of absorption in the gas path, and modeling of the spectral resolution of the spectrometer, since the detection system will average stronger and weaker lines. Although an attempt was made to compare the model to the low resolution data, it was quickly decided that since more spectral resolution is available in newer Ocean Optics spectrometers there was no compelling reason to work at the resolution shown in Figure 29.

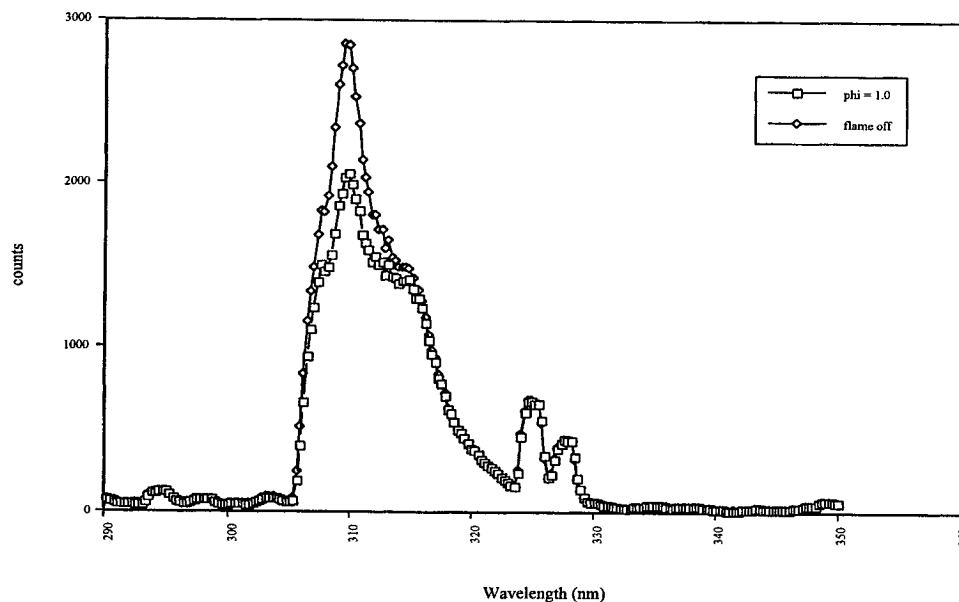


Figure 29: OH Spectra obtained with the PC 1000 in a Laboratory Flame

Field Test of the Absorption Measurement Instrumentation

During March and April of 1996, a modification to the initial contract was requested by NASA. to restructure the program so that Task 4 was changed from combustor simulator measurements made at UTRC to measurements made at Lewis Research Center's Propulsion System Laboratory (PSL) in the exhaust of a Williams gas turbine engine (WGTE). Considerable effort was expended to prepare for participation in the test program at the PSL. A very brief summary of those activities follows.

After preliminary discussions with other participants in the test program (Aerodyne, UMR and Lewis personnel) and a visit to the PSL facility, a laboratory simulation of the anticipated requirements necessary for deployment of the absorption measurement instrumentation at the PSL facility was setup at UTRC. Briefly this consisted of a flat flame burner to simulate the WGTE, an arrangement of UV lens and a reflector that allowed a two-pass working pathlength between 4 and 6 meters, coupling of the resonant UV source and

spectrometer through 10 meter UV optical fibers, remote control (120 meter cable) of the data acquisition computer with a lap top computer, and provisions to switch between the NO and OH resonant source in a matter of minutes. In addition, coordination with PSL facility personnel to determine the specifics of the NASA support and participation in several group telephone conference calls (LeRC, UMR and ARI personnel) to discuss deployment and test matrix issues was also performed. The instrumentation was shipped to LeRC on June 12, 1996.

Unfortunately the instrumentation was never deployed. In the end, an inability of Williams, UTRC, and NASA to agree on the details of a non-disclosure statement prohibited UTRC from participation in the test program. Issues that were thought to have been resolved at the outset were, in fact, not resolved. The equipment was returned to UTRC without being used.

Conclusions

Ultraviolet, line-of-sight, resonant absorption spectrometry has been demonstrated for the measurement of nitric oxide (NO) and hydroxyl radical (OH) at pressures up to 30 atmospheres. The overall agreement between model predictions and measurements for NO was within 25%. This agreement was dependent on the accuracy of the temperature measurements and subsequent estimation of thermocouple radiative losses. Similarly, the overall agreement between OH predictions and measurements was reasonable. The OH agreement was also dependent on the accuracy of the radiation corrected temperature measurements and equilibrium model predictions based on those temperature measurements, since probe sampling cannot be used to measure this species.

The impact of line center shifting on the interpretation of the data was determined to be insignificant on the accuracy of both the NO and OH measurement up to 30 atmospheres. It should be noted that this may not be true for this line-of-sight method in the 50 to 60 atmosphere range. Also, it was determined that the reference method used during the previous FAA funded study for NO is adequate for dealing with the continuum absorption produced by hot oxygen at pressures up to 30 atmospheres.

Finally, the line-of-sight, resonant absorption technique is a viable method for measuring NO and OH at the exit of current and potentially next generation jet combustors and engines.

New Technology

1. A commercially available miniature fiber optic plug-in spectrometer (PC1000) from Ocean Optics was evaluated in this program. This low-cost spectrometer is based on a 1024-element linear CCD-array which is coupled to a fiber optic and arranged on a half-length, 500 kHz ISA-bus A/D card that conveniently installs into an ISA-bus slot in a standard personal computer. The device was found to be rugged, reliable, and easy to use. Spectral resolution approaches that of a standard laboratory spectrometer in the currently available models. This instrument demonstrated that technology advances in the miniaturization of spectrometers offer viable options for future field measurements.
2. An existing NO spectroscopic model was modified and validated for line center shifting up to 30 atm.
3. A new OH spectroscopic model is now available.

Suggestions for Future Activities

The work presented in this report lays a solid background for the direction of several follow-on activities:

- Extend the optical measurements to 60atm
Data of this kind are non-existent at the current time. We have found using UTRC funds that the premixed flame is stable at equivalence ratios as low as 0.8 at 60atm allowing a range of data to be acquired for kinetic model validation. Accurate temperature profiles would also be acquired.
- Acquire extractive gas sampling probe measurements at 60atm
These data would also be a first and require a relatively small effort
- Acquire high resolution OH data
Further validation of the OH model requires higher resolution data in order to more easily isolate the effect of variables in the calculation.
- Continue development of a portable instrument
The limited work done in this program indicates excellent potential for a high quality low cost field instrument.

References

- Bradley, D., Entwistle, A.G., "Determination of the Emissivity, for Total Radiation, of Small Diameter Platinum-10% Rhodium Wires in the Temperature Range 600-1450C", *British Journal of App. Phys.*, Vol. 12, December 1961.
- Carter, D, King, G.B., and Laurendeau, N.M., "Saturated Fluorescence Measurements of the Hydroxyl Radicals in Laminar High-Pressure Flames", NASA Contractor Report 185218, 1990.
- Chang, A.Y., DiRosa, M.D. and Hanson, R.K., "Temperature Dependence of Collision Broadening and Shift in the NO A←X(0,0) Band in the Presence of Argon and Nitrogen", *J. Quant. Spectrosc. Radiant. Transfer*, **47**, 375-390, 1992.
- Colket, M.B., Sangiovanni, J.J., Tredway, W.K., Schmidt, W.R., Knight, B.A., and Snider, T.R.; "Topical Report on Reactor Fabrication and Catalyst Selection for Hybrid Combustion", Report No. UTRC 970373-12 for GRI Contract No. 5092-238-2389, October 1993.
- DiRosa, M.D., Klavuhn, K.G., and Hanson, R.K., "LIF Spectroscopy of NO and O2 in High-Pressure Flames", *Combust. Sci. and Tech.*, **118**, pp. 257-283, 1996.
- DiRosa, M.D. and Hanson, R.K. "Collisional Broadening and Shift of NO g(0,0) Absorption Lines by O2 and H2O at High Temperatures", *J. Quant. Spectrosc. Radiat. Transfer*, **52**, 515-529. 1994a.
- DiRosa, M.D. and Hanson, R.K. "Collisional Broadening and Shift of NO g(0,0) Absorption Lines by O2 and H2O at 295K", *J.Molec. Spectrosc.*, **164**, 97-117, 1994b.
- Davis, M.G., McGregor, W.K. and Few, J.D., "Utilizing the Resonance Line Absorption Technique to Determine the Collisional Broadening Parameters of a Diatomic Molecule: NO γ -Bands as an Example", *J. Quant. Spectrosc. Radiant. Transfer*, **16**, 1109-1118, 1976.
- Few, J.D., McGregor, W.K., and Glassman, H.N., "Resonance Absorption Measurements of NO Concentration in Combustor Exhausts", *AIAA Progress in Astronautics and Aeronautics - Experimental Diagnostics in Gas Phase Systems*, B.T. Zinn, editor, AIAA Press, Princeton, NJ, 1977.
- Goldman, A. and Gillis, J.R., "Spectral Line Parameter for the A² Σ -X² π (0,0) band of OH for Atmospheric and High Temperatures", *J. Quant. Spectrosc. Radiant. Transfer*, **25**, 111, 1981.
- Howard, R.P., et. al., "Nonintrusive Nitric Oxide Density Measurements in the Effluent of Core-Heated Airstreams", *AIAA 21st Fluid Dynamics, Plasma Dynamics and Lasers Conference*, AIAA-90-1478, Seattle WA, June 18-20, 1990.
- Meinel, H. and Just, Th., "Measurement of NO_x Exhaust Emissions by a New NDUV Analyzer", *AIAA Progress in Astronautics and Aeronautics - Experimental Diagnostics in Gas Phase Systems*, B.T. Zinn, editor, AIAA Press, Princeton, NJ, 1977.

- Rea, E.C., "Rapid-tuning Laser Wavelength Modulation Spectroscopy with Applications in Combustion Diagnostics and OH Line Shape Studies", Ph.D. Thesis, Stanford University, 1991.
- Rea, E.C., Chang, A.Y. and Hanson, R.K., "Collision Broadening of the $A^2\Sigma^+-X^2\pi$ band of OH by H_2O and CO_2 in Atmospheric-Pressure Flames", *J. Quant. Spectrosc. Radiant. Transfer*, **41**, 29, 1989.
- Rea, E.C., Chang, A.Y. and Hanson, R.K., "Shock Tube Study of Pressure Broadening of the $A^2\Sigma^+-X^2\pi$ band of OH by Ar and N_2 ", *J. Quant. Spectrosc. Radiant. Transfer*, **37**, 117, 1987.
- Roberts, W.L., et. al., "Measurement and Prediction of Nitric Oxide Concentration in the HYPLUSE Expansion Tube Facility", 18th AIAA Aerospace Ground Testing Conference, Colorado Springs, CO, June 20-23, 1994.
- Shirinzadeh, B., Bakalyar, D.M. and Wang, C.C., "Measurements of Collision Induced Shift and Broadening of the Ultraviolet Transitions of OH", *J. Chem. Phys.* **82**, 2877, 1985.
- Stark, G., Brault, J.W. and Abrams, M.C., "Fourier-Transform Spectra of the $A^2\Sigma^+-X^2\pi$ $\Delta v=0$ bands of OH and OD", *J. Opt. Soc. Am. B* **11**, 3, 1994.
- Zabielski, M.F., Dodge, L.G., Colket, M.B., and Seery, D.J.; "Nitric Oxide Measurement Study: Comparison of Optical and Probe Methods, Task III Report. Prepared by UTRC for DOT-FAA under Contract FA77WA-4081, January 1980.



REPORT DOCUMENTATION PAGE

Form Approved
OMB No. 0704-0188

Public reporting burden for this collection of information is estimated to average 1 hour per response, including the time for reviewing instructions, searching existing data sources, gathering and maintaining the data needed, and completing and reviewing the collection of information. Send comments regarding this burden estimate or any other aspect of this collection of information, including suggestions for reducing this burden, to Washington Headquarters Services, Directorate for Information Operations and Reports, 1215 Jefferson Davis Highway, Suite 1204, Arlington, VA 22202-4302, and to the Office of Management and Budget, Paperwork Reduction Project (0704-0188), Washington, DC 20503.

1. AGENCY USE ONLY (Leave blank)		2. REPORT DATE December 1998	3. REPORT TYPE AND DATES COVERED Final Contractor Report	
4. TITLE AND SUBTITLE Development of UV Optical Measurements of Nitric Oxide and Hydroxyl Radical at the Exit of High Pressure Gas Turbine Combustors			5. FUNDING NUMBERS WU-538-08-12-00 NAS3-27593	
6. AUTHOR(S) D.S. Liscinsky, B.A. Knight, and J.A. Shirley				
9. SPONSORING/MONITORING AGENCY NAME(S) AND ADDRESS(ES) United Technologies Research Center East Hartford, Connecticut 06108			8. PERFORMING ORGANIZATION REPORT NUMBER E-11498	
9. SPONSORING/MONITORING AGENCY NAME(S) AND ADDRESS(ES) National Aeronautics and Space Administration Lewis Research Center Cleveland, Ohio 44135-3191			10. SPONSORING/MONITORING AGENCY REPORT NUMBER NASA CR-1998-208869	
11. SUPPLEMENTARY NOTES Project Manager, Chowen Chou Wey, U.S. Army Research Laboratory, NASA Lewis Research Center, organization code 0300, (216) 433-8357.				
12a. DISTRIBUTION/AVAILABILITY STATEMENT Unclassified - Unlimited Subject Category: 01 This publication is available from the NASA Center for AeroSpace Information, (301) 621-0390.			12b. DISTRIBUTION CODE Distribution: Nonstandard	
13. ABSTRACT (Maximum 200 words) Measurements of nitric oxide (NO) and hydroxyl radical (OH) have been made in a laboratory flat flame at pressures up to 30 atm using line-of-sight resonant absorption. Data are reported at equivalence ratios of 0.98 and 1.3 and pressures of 1, 5, 10, 20 and 30 atm. The performance of the <i>in-situ</i> UV absorption technique with assessed at these elevated pressures by comparing the measured absorption with those predicted by detailed theoretical spectroscopic models for NO and OH. Previous to this experiment the resonant models had not been verified at pressures greater than two atmospheres. Agreement within 25% was found between the measurements and predictions with only slight modification of the existing models for both NO and OH to account for line center shifting and pressure broadening. Continuum interference of hot oxygen (O ₂) on the NO absorption spectra was not significant in the interpretation of the data. The optical methods used in this study are distinct from laser-based diagnostics such as laser induced fluorescence and, hence, have the potential to provide independent verification of the laser-based measurements. The methodology is also of sufficient simplicity to be hardened into a portable optical measurement system that can be deployed in gas turbine engine test cells. A miniature fiber optic couple portable instrument is described.				
14. SUBJECT TERMS Combustor emissions measurement; Optical measurement			15. NUMBER OF PAGES 40	
			16. PRICE CODE A03	
17. SECURITY CLASSIFICATION OF REPORT Unclassified	18. SECURITY CLASSIFICATION OF THIS PAGE Unclassified	19. SECURITY CLASSIFICATION OF ABSTRACT Unclassified	20. LIMITATION OF ABSTRACT	

NSN 7540-01-280-5500

Standard Form 298 (Rev. 2-89)
Prescribed by ANSI Std. Z39-18
298-102